

Quantum Second Virial Coefficient Calculation for the ^4He Dimer on a Recent Potential

Éderson D'Martin Costa,^a Nelson H. T. Lemes,^a Márcio O. Alves,^b
Rita C. O. Sebastião^b and João P. Braga^{*,b}

^aInstituto de Química, Universidade Federal de Alfenas,
Rua Gabriel Monteiro da Silva, 700, Centro, 37130-000 Alfenas-MG, Brazil.

^bDepartamento de Química, Universidade Federal de Minas Gerais,
Av. Antônio Carlos, 6627, Pampulha, 31270-010 Belo Horizonte-MG, Brazil.

Este trabalho concentra-se no cálculo do segundo coeficiente virial quântico, a partir de um potencial desenvolvido recentemente. Este coeficiente foi determinado com 4-5 algarismos significativos na faixa de temperatura de 3 a 100 K. Nossos resultados estão dentro do erro experimental. Três contribuições para o valor total deste coeficiente são o espalhamento quântico (contribuição de estados no contínuo), o estado ligado (contribuição de estados discretos) e o gás ideal quântico; discutimos estas contribuições separadamente. A contribuição mais importante é do espalhamento quântico, enquanto que as contribuições menores são dos estados discretos. Uma análise da sensibilidade foi realizada em função da temperatura para um parâmetro na região de curto alcance do potencial e para três parâmetros na região de longo alcance do potencial. Para ambas as temperaturas consideradas, 10 e 100 K, o coeficiente de dispersão C_6 foi o mais significativo, e o termo dispersão C_{10} foi o menos significativo para o resultado total. Em geral, a precisão exigida para descrever os potenciais diminui com o aumento da temperatura. A precisão total e a relação dos parâmetros com os erros experimentais são discutidas.

This paper focuses on the calculation of the quantum second virial coefficient, under a recently developed potential. This coefficient was determined to within 4-5 significant figures in the temperature range from 3 to 100 K. Our results are within experimental error. The three contributions to the overall value of the coefficient are the quantum scattering (continuum state contribution), the bound state (discrete state contribution) and the quantum ideal gas; we discuss these contributions separately. The most significant contribution is from the scattering states, whereas the smaller contributions are from the discrete states. A sensitivity analysis was performed as a function of temperature for one parameter in the short-range region of the potential and for three parameters in the long-range regions of the potential. For both temperatures considered, 10 and 100 K, the C_6 dispersion coefficient was the most significant, and the C_{10} dispersion term was the least significant to the overall result. In general, the precision required to describe the potential decays as the temperature increases. The overall accuracy and the relationship of the parameters to the experimental errors are discussed.

Keywords: quantum virial, helium-helium, scattering phase shift.

Introduction

A quantum second virial coefficient calculation provides important information that is necessary for analyzing model potentials, for this calculation involves low temperature data.¹ These potential energy function can be obtained by a direct procedure, such as fitting parameters to experimental data, or, conversely, by

an inverse problem treatment, in which experimental properties are treated first.²⁻⁵ The potential refinement is very important in chemistry and is performed whenever new reliable data become available. Accurate values of helium properties, such as the low-temperature experimental virial coefficient, can be determined⁶⁻⁸ and experimental $^4\text{He}_2$ dimers can be identified.⁹⁻¹⁵ Thus, a comparison between theory and experiment is an important test for the quality of the interatomic He potential.

*e-mail: jpbraga@netuno.lcc.ufmg.br

Several He-He intermolecular potentials are discussed in the literature.¹⁶⁻²⁰ The most recent potential has not been tested against thermodynamic and transport property data,²¹ such as the quantum second virial coefficients. In the present work, a study of this recent potential was conducted using second virial coefficient data at low temperature. The quantum virial coefficient can be determined by evaluating the quantum ideal gas term, the scattering phase shift dependence on angular momentum²²⁻²⁹ and the bound states by Levinson's theorem.²⁵⁻²⁶

This low-temperature second virial coefficient calculation is an important step to test the quality of the potential under consideration. Together with this quantum calculation, a sensitivity analysis on the dispersion coefficients is also performed. This test is very important, especially in low energy conditions when the potential parameters are more sensitive. The results obtained in the present work will be compared to experimental data for the helium-helium system.²²⁻²⁴

Experimental

The partial wave method

A numerical solution to the Schrödinger equation is the first step to providing information about the quantum virial coefficient. In the scattering process, the Schrödinger equation can be written as

$$\left[\frac{d^2}{dr^2} + k^2 - \frac{2\mu E_p(r)}{\hbar^2} - \frac{l(l+1)}{r^2} \right] \psi_l(r) = 0, \quad (1)$$

where $k^2 = 2\mu E/\hbar^2$, l is the angular momentum, μ is the reduced mass and E is the energy of the relative motion. After the collision process, the scattered wave function is

$$\psi_l(r) = A \sin \left(kr - \frac{l\pi}{2} + \delta_l \right). \quad (2)$$

The phase shift, δ_l , carries all of the necessary information to describe the scattering, as it represents a phase that is accumulated along the scattering process with respect to a free particle. If no potential were present, the phase shift would be zero. The phase shift was calculated by the renormalized Numerov method, which is a very robust numerical procedure for solving equation 1.³⁰ Riccati-Bessel functions were used to match Schrödinger equation solutions at a maximum scattering coordinate.³¹ At this point, wavefunction continuity are imposed and the scattering matrix (or phase shift) can be established.³²

Quantum virial coefficient

The equation of state for the helium system can be represented by $p/k_B T = r + B(T)\rho^2$, in which r is the density and $B(T)$ is the second virial coefficient. The classical second virial coefficient is not appropriate to describe the helium equation of state at temperatures lower than 100 K.²² Instead, the exact quantum second virial coefficient expression relating the phase shift and the energy of bound state is used for an accurate system description.^{6,23,24} The molar virial expansion is represented in the form

$$B(T) = B_{\text{ideal}} + B_{\text{bound}} + B_{\text{phase}} \\ = - \left(\frac{4\pi\hbar^2}{\mu k_B T} \right)^{3/2} \left[\frac{1}{16} + \left(e^{-\frac{\epsilon}{k_B T}} - 1 \right) + \frac{2}{\pi q_0^2} \int_0^\infty e^{-q^2/q_0^2} G(q) q dq \right] \quad (3)$$

in which ϵ is the He₂ binding energy for zero angular momentum, k_B is Boltzmann's constant and

$$G(q) = \sum_{\text{even}} (2l+1) \delta_l(q) \\ q^2 = 2\mu\sigma^2 E / \hbar^2 \\ q_0^2 = 2\mu\sigma^2 k_B T / \hbar^2 \quad (4)$$

with $\sigma = 2.556 \text{ \AA}$. The dimensionless variables q and q_0 were conveniently introduced in formulating the problem and are related to the collision energy and temperature, respectively. For further comparison, if $q = 1$ for the system under consideration, the collision energy will be $E = 1.60 \times 10^{-4} \text{ eV}$. Moreover, $q_0 = 1$ will correspond to $T = 1.85 \text{ K}$. Other transformations can be obtained with this reference. As the energy increases, the phase shift will gradually approach zero, and the integral term in equation 3 will converge.

For the ⁴He dimer, the ideal part of the second virial coefficient, B_{ideal} , considers the Bose statistics, and no intermolecular forces are considered.³³ This term is important at low temperature and approaches zero at higher temperature. The inclusion of the discrete energy levels, with only one rovibrational state for He₂ in the partition function, gives rise to the second term in equation 3, B_{bound} . A contribution from the scattering states comes from the third term, B_{phase} , in which the phase shift has to be considered. This term is the most important one in establishing the second virial coefficient for the helium system.²²

Potential energy function

For the description of the system, an accurate potential developed by Varandas²¹ was employed. This potential is given by a Hartree-Fock short-range energy and a long-range correlation energy, $E_p(R) = V_{\text{HF}}(R) + V_{\text{cor}}(R)$, in which,

$$V_{\text{HF}}(R) = D \left(1 + \sum_{i=1}^4 a_i (R - R_e)^i \right) \exp(-\gamma(R - R_e)) \quad (5)$$

and

$$V_{\text{cor}}(R) = - \sum_{n=6,8,10-16} C_n \chi_n(R) R^{-n} \quad (6)$$

are used to define the potential. The function, $\chi_n(R)$, is

$$\begin{aligned} \chi_n(R) &= [1 - \exp(-A_n R / \rho - B_n R^2 / \rho^2)]^n \\ A_n &= \alpha_0 n^{-\alpha_1} \\ B_n &= \beta_0 n^{-\beta_1} \end{aligned} \quad (7)$$

The value in atomic units of the damping function coefficients are: $\rho = 10.9424025$, $\alpha_0 = 16.36606$, $\alpha_1 = 0.70172$, $\beta_0 = 17.19338$ and $\beta_1 = 0.09574$. The other necessary parameters to determine the potential are given in Table 1.

Table 1. Parameters for the helium potential in atomic units²¹

V_{HF} parameters		Dispersion coefficients	
D	$2.909582149142803 \times 10^{-5}$	C_6	1.4646
a_1	$-2.677678262034801 \times 10^{-1}$	C_8	14.112
a_2	$2.345720241868299 \times 10^{-2}$	C_{10}	178.13
a_3	$1.459174818996908 \times 10^{-2}$	C_{11}	-76.7
a_4	$1.237617600368155 \times 10^{-5}$	C_{12}	3093
R_e	5.60323206384019	C_{13}	-3806.0
γ	2.17613250152118	C_{14}	72016
		C_{15}	-171000.0
		C_{16}	2276994

Data in the literature¹⁶⁻²⁰ show that the He dimer potential well at 10.9 K and a nuclear equilibrium distance of 2.97 Å only support a single bound rovibrational state with a binding energy of approximately -1.176 mK,³⁴ which is the weakest bound state ever discovered. Due to this extremely weak interaction, the wave function must be delocalized over a large intermolecular distance. The mean intermolecular distance for He at the ground state is approximately 50 Å.⁹⁻¹⁵

The minimum energy value ($D = 11.0$ K) and the equilibrium distance ($R_e = 2.965$ Å) predicted by the potential used here are in agreement with previous results in the literature.¹⁶⁻²¹ This proposed potential energy curve is investigated, by comparing the calculated exact quantum second virial coefficient with the experimental results at low temperatures.

The quantum scattering calculation

Calculation of the quantum second virial coefficient requires a solution to Schrödinger's equation and, after appropriate boundary conditions, the quantum phase shift calculation. The renormalized Numerov algorithm that propagates the ratio of wave functions was used to calculate the scattering matrix from which the phase shift was found.³⁰ Propagating the ratio of the wave function at two consecutive points, such as $\frac{\Psi(r+h)}{\Psi(r)}$ is the essential idea behind this renormalized method; here, h is the integration step size. This procedure will provide a very stable propagator, even into the classically forbidden regions. A critical analysis of this method appears in the literature.³⁵

Levinson's theorem relates the zero energy phase shift to the number of bound states supported by the potential using

$$\delta_l(q \rightarrow 0) = n_l \pi \quad (8)$$

Here, n_l is the number of bound states for the given angular momentum.³⁵ The $^4\text{He}_2$ molecule was experimentally detected by several groups.⁹⁻¹⁵ For $l \geq 1$ the helium molecule was not detected, a fact that was also confirmed numerically in this study.

For large angular momentum states, the centrifugal term will dominate the collision process, and the scattering process will occur with negligible changes in potential energy. At this point, phase shift will decrease to zero. Therefore, the quantity $G(q)$, which is necessary to calculate the second virial coefficient, will converge for a maximum angular momentum, l_{max} .^{6,23} By angular momentum conservation, one can estimate this maximum at $l_{\text{max}} \approx kR_{\text{max}}$, in which R_{max} is the potential range. The quantity l_{max} is the maximum angular momentum required to achieve cross section convergence.

The quantity $g(q) = G(q)e^{-q^2/q_0^2}$ is shown in Figure 1, using the Varandas potential. The maximum angular momentum in the range of $20 < l_{\text{max}} < 80$ gives a convergence of at least 4(lower temperatures)-5(higher temperatures) significant figures for energies in the range $0 < q < 80$. The $G(q)$ curve presents a primary peak near $q = 0$, which is predicted by Levinson's theorem. As observed for temperatures under 30 K, the integration process must be performed until $q = 14$, which is the convergence point for the energy. The phase shifts were calculated at intervals of $\Delta q = 0.005$. Numerical integration was performed using Simpson's method together with a cubic spline interpolator.^{36,37} Integrated results were confirmed to be within 4-5 significant figures.

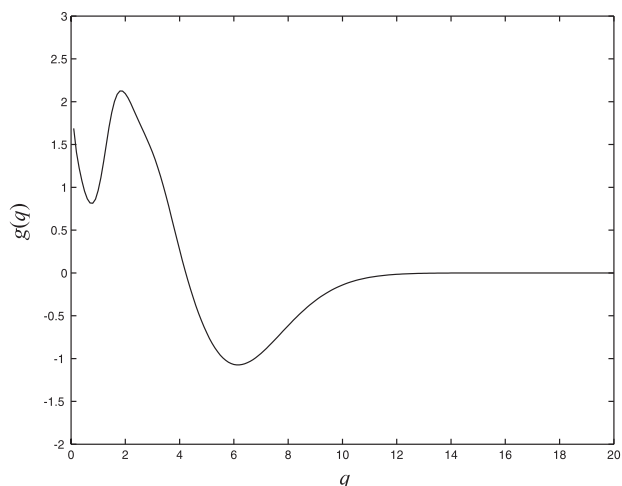


Figure 1. A plot of the function $g(q) = G(q)qe^{-q^2/q_0^2}$ at $T = 30$ K.

Results and Discussions

The present calculation of the quantum second virial coefficient was performed with 4-5 significant figures, and the results are shown in Table 2. A comparison is made with experimental and theoretical calculation. The second virial coefficient error calculated in the present work is within $0.1 \text{ cm}^3 \text{ mol}^{-1}$ for temperatures above 10 K, but this result increases to $0.63 \text{ cm}^3 \text{ mol}^{-1}$ for $T = 3$ K. Guided by the experimental error of $0.6 \text{ cm}^3 \text{ mol}^{-1}$ for lower temperatures, one may conclude that the potential used in the present calculation is appropriate in this temperature range.^{8,38}

Table 2. Second virial coefficients for ⁴He in units of $\text{cm}^3 \text{ mol}^{-1}$

T, K	Experimental ⁸	This work
3.0	-120.3	-119.67
4.0	-85.3	-84.70
5.5	-56.9	-56.55
7.0	-40.8	-40.56
9.0	-27.69	-27.56
11.0	-19.38	-19.31
13.0	-13.65	-13.60
15.0	-9.47	-9.43
17.5	-5.61	-5.58
20.0	-2.75	-2.71
29.0	3.35	3.41
40.0	6.89	6.985
41.0	7.11	7.206
45.0	7.88	7.982
60.0	9.74	9.855
75.0	10.74	10.852
90.0	11.32	11.427
100.0	11.58	11.675

Term contribution

We discuss the individual contributions to the second virial coefficient expansion in equation (3). The first term is a Bose-Einstein ideal gas contribution, the second term is the bound state contribution, and the third term is related to atomic interaction as determined by the phase shift information.

The quantum ideal gas term,³³

$$-\left(\frac{4\pi\hbar^2}{\mu k_B T}\right)^{3/2} \frac{1}{16}, \quad (9)$$

is significant at low temperature and decreases in importance as the temperature is increased. For example, this term contributes approximately 11% at 3 K and 0.7% at 100 K. Due to the Bose-Einstein statistics, this contribution is always negative for the second virial coefficient. For room temperature, this term can be neglected.

The existence of a ⁴He diatomic molecule for the potential under consideration makes it necessary to consider the bound state term,

$$-\left(\frac{4\pi\hbar^2}{\mu k_B T}\right)^{3/2} \left(e^{-\frac{\epsilon}{k_B T}} - 1\right) \quad (10)$$

This contribution to virial expansion represents 0.07% at 3 K and decreases at large temperatures to $10^{-4}\%$ at 100 K; these values are much smaller than the ideal quantum gas correction. In fact, error in the bound state energy will not have a considerable effect on the second virial coefficient data.

However, the phase shift contribution to virial calculation,

$$-\left(\frac{4\pi\hbar^2}{\mu k_B T}\right)^{3/2} \frac{2}{\pi q_0^2} \int_0^\infty e^{-q^2/q_0^2} G(q) q dq \quad (11)$$

is significant; therefore, quantum virial coefficient data at low temperatures are a good test of novel potential functions. For example, B_{phase} at 3 K represents 88.6% of the total contribution to the coefficient. In Table 3, we show the individual contributions of these three terms from 3 K to 100 K.

Sensitivity analysis

An important issue involves the question of how the potential energy function has to be to reproduce a desired property. The answer is provided by the sensitivity analysis.³⁹ This question was analyzed, and the results

Table 3. Calculated quantum second virial coefficient contribution terms in $\text{cm}^3 \text{mol}^{-1}$

T	B	B_{phase}	B_{ideal}	B_{bound}
3.0	-119.67	-105.97	-13.614	-8.5402×10^{-2}
4.0	-84.698	-75.814	-8.8424	-4.1601×10^{-2}
5.5	-56.552	-51.049	-5.4842	-1.8764×10^{-2}
7.0	-40.563	-36.733	-3.8196	-1.0268×10^{-2}
9.0	-27.564	-24.939	-2.6200	-5.4778×10^{-3}
11.0	-19.307	-17.365	-1.9390	-3.3169×10^{-3}
13.0	-13.604	-12.093	-1.5092	-2.1845×10^{-3}
15.0	-9.4351	-8.2159	-1.2177	-1.5275×10^{-3}
17.5	-5.5823	-4.6150	-0.96628	-1.0390×10^{-3}
20.0	-2.7118	-1.9202	-0.79089	-7.4409×10^{-4}
29.0	3.4108	3.8640	-0.45296	-2.9390×10^{-4}
40.0	6.9847	7.2644	-0.27962	-1.3154×10^{-4}
41.0	7.2062	7.4758	-0.26945	-1.2366×10^{-4}
45.0	7.9821	8.2165	-0.23434	-9.7986×10^{-5}
60.0	9.8550	10.007	-0.15221	-4.7732×10^{-5}
75.0	10.852	10.960	-0.10891	-2.7324×10^{-5}
90.0	11.427	11.509	-0.082851	-1.7321×10^{-5}
100.0	11.675	11.746	-0.070739	-1.3299×10^{-5}

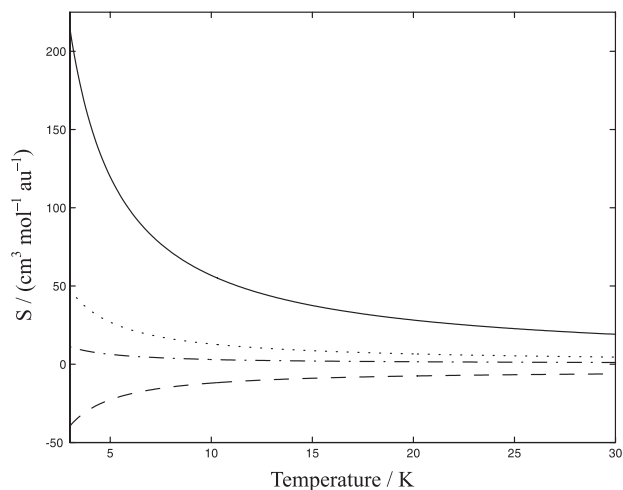
are shown in Table 4. Accordingly, the uncertainties established are greater than those established with the Varandas potential.²¹

Table 4. Acceptable parameter deviation for $\Delta B = 0.01$ in $\text{cm}^3 \text{mol}^{-1}$ and atomic units

	Parameter	Sensitivity	Deviation	Error ²¹
$T = 10 \text{ K}$	C_6	50	2×10^{-4}	10^{-12}
	C_8	10	10^{-3}	10^{-8}
	C_{10}	1	10^{-2}	10^{-6}
	γ	10	10^{-3}	–
$T = 100 \text{ K}$	C_6	10	10^{-3}	10^{-12}
	C_8	1	10^{-2}	10^{-8}
	C_{10}	1	10^{-2}	10^{-6}
	γ	5	2×10^{-3}	–

The sensitivity of the second virial coefficient is greater for the C_6 dispersion term and smaller for the C_8 and C_{10} terms; these results are presented in Figure 2. The short-range γ Born-Mayer type parameter importance, shown in the figure, is as relevant as the C_8 term. The temperature dependence of the potential parameters is the important information that is obtained from Figure 2. It is clear that all terms become less important as the temperature is increased.

The second virial coefficient experimental error will be assumed to be $\pm 0.01 \text{ cm}^3 \text{mol}^{-1}$,⁸ which is below the average experimental error. One might then ask what

**Figure 2.** Parametric sensitivity analysis for C_6 (–), C_8 (···), C_{10} (– –) and γ (– · –) in atomic units and $\text{cm}^3 \text{mol}^{-1}$.

will the allowed error in the potential parameter be, at a given temperature, to give this experimental error. As stated in the potential model used here,²¹ the errors in the dispersion coefficient C_6 , C_8 and C_{10} are 10^{-12} , 10^{-8} and 10^{-6} , respectively. This result is not compatible with the sensitivity of the dispersion coefficient, as presented in Table 4. The variation in these parameters, even for 100 K, is well below the data used in the construction of the potential model.²¹ For lower temperatures, the variation in these parameters is more restricted but still below the assumed experimental error.

A family of potential energy curves is an acceptable method used to reproduce the second quantum virial coefficient. For example, the potential used in the present work is similar to other potentials in the literature,¹⁶ and the calculated quantum second virial coefficient will provide data within experimental error if these potentials are used; we emphasize this point in Table 2. Experimental error provides a rule to be followed in modeling potential energy function. Therefore, if accurate information is used, such as the quantum second virial data, important restriction on the potential model is imposed.

Conclusions

Quantum second virial coefficient for the $^4\text{He}_2$ system were calculated in the present work for a novel potential over the temperature range from 3 to 100 K. Calculations in this temperature range showed classical or semi-classical behavior that were not sufficient to adequately describe the second virial data. Our results are in agreement with experimental errors. For example, the difference between our theoretical results and the experimental data are $0.63 \text{ cm}^3 \text{mol}^{-1}$ for $T = 3 \text{ K}$ and $0.095 \text{ cm}^3 \text{mol}^{-1}$ for $T = 100 \text{ K}$.

Contributions from the bound state term, the Bose-Einstein interaction and the phase shift were discussed. The first two terms showed a small influence on this coefficient. For example, at 3 K, the bound state contribution is 0.07% and the Bose-Einstein is 11%, while at the same temperature, the phase shift term contributes 89% to the total second virial coefficient.

Under the inverse problem theory framework, a potential parameter sensitivity analysis was also studied. The calculated uncertainties in the parameter were, in fact, greater than the precision used to construct the potential used in the present calculation. For example, to be within experimental error, the dispersion coefficient C_6 can have uncertainty as small as 10^{-4} au, which is well above the theoretical calculation of 10^{-14} au.

Theoretical calculations with the potential function proposed by Varandas and used in the present work are within experimental error. In fact, it was difficult to select the best potential that describes helium-helium interaction at low temperatures. Sensitivity analysis has shown that the precision in the potential parameters is beyond that which is required to reproduce the experimental quantum second virial coefficient; therefore, a set of potentials is acceptable.

Acknowledgments

We would like to thank CNPq, CAPES and FAPEMIG for financial support.

References

1. Pethick, C. J.; Smith, H.; *Bose-Einstein Condensation in Dilute Gases*; Cambridge University Press: Cambridge, 2002.
2. Lemes, N. H. T.; Braga, J. P.; Belchior, J. C.; *Chem. Phys. Lett.* **1998**, *296*, 233.
3. Braga, J. P.; de Almeida, M. B.; Braga, A. P.; Belchior, J. C.; *Chem. Phys.* **2000**, *260*, 347.
4. Sebastião, R. C. O.; Lemes, N. H. T.; Virtuoso, L. S.; Braga, J. P.; *Chem. Phys. Lett.* **2003**, *378*, 406.
5. Lemes, N. H. T.; Sebastião, R. C. O.; Braga, J. P.; *Inverse Probl. Sci. En.* **2006**, *14*, 581.
6. Colclough, A. R.; *Metrologia* **1979**, *15*, 183.
7. Kessler, W. D.; Osborne, D. V.; *J. Phys. C: Solid St. Phys.* **1980**, *13*, 2097.
8. Steur, P. P. M.; Duriex, M.; McConville, G. T.; *Metrologia* **1987**, *24*, 69.
9. Luo, F.; McBane, G. C.; Kim, G.; Giese, C. F.; Gentry, W. R.; *J. Chem. Phys.* **1993**, *98*, 3564.
10. Meyer, E. S.; Mester, J. C.; Silveira, I. F.; *J. Chem. Phys.* **1994**, *100*, 4021.
11. Luo, F.; McBane, G. C.; Kim, G.; Giese, C. F.; Gentry, W. R.; *J. Chem. Phys.* **1994**, *100*, 4023.
12. Schöllkopf, W.; Toennies, J. P.; *Science* **1994**, *266*, 1345.
13. Luo, F.; Giese, C. F.; Gentry, W. R.; *J. Chem. Phys.* **1996**, *104*, 1151.
14. Schöllkopf, W.; Toennies, J. P.; *J. Chem. Phys.* **1996**, *104*, 1155.
15. Focsa, C.; Bernath, P. F.; Colin, R.; *J. Mol. Spectrosc.* **1998**, *191*, 209.
16. Przybytek, M. and Cencek, W.; Komasa, J.; Szalewicz, K.; *Phys. Rev. Lett.* **2010**, *104*, 183003.
17. Hurly, J. J.; Mehl, J. B.; *J. Res. Natl. Stand. Technol.* **2007**, *112*, 75.
18. Jeziorska, M.; Cencek, W.; Patkowski, K.; Jeziorski, B.; Szalewicz, K.; *J. Chem. Phys.* **2007**, *127*, 124303.
19. Janzen, A. R.; Aziz, R. A.; *J. Chem. Phys.* **1997**, *107*, 914.
20. Janzen, A. R.; Aziz, R. A.; *J. Chem. Phys.* **1995**, *103*, 9626.
21. Varandas, A. J. C.; *J. Phys. Chem., A* **2010**, *114*, 8505.
22. Boyd, M. E.; Larsen, S. Y.; Kilpatrick, J. E.; *J. Chem. Phys.* **1969**, *50*, 4034.
23. Kilpatrick, J.; Keller, W.; Hammel, E.; Metropolis, N.; *Phys. Rev.* **1954**, *94*, 1103.
24. Kihara, T.; *Rev. Mod. Phys.* **1955**, *27*, 412.
25. Bernstein, B. R. In *Atom-Molecule Collision Theory, A Guide For The Experimentalist*; Bernstein, B. R., eds.; Plenum Press: New York, 1979.
26. Murrell, J. N.; Bosanac, S. D. *Introduction to the theory of atomic and molecular collisions*; John Wiley & Sons: New York, 1989.
27. Siska, P. E.; Parson, J. M.; Schafer, T. P.; Lee, Y. T.; *J. Chem. Phys.* **1971**, *55*, 5762.
28. Farrar, J. M.; Lee, Y. T.; *J. Chem. Phys.* **1972**, *56*, 5801.
29. Burgmans, A. L. J.; Farrar, J. M.; Lee, Y. T.; *J. Chem. Phys.* **1976**, *64*, 1345.
30. Johnson, B. R.; *J. Chem. Phys.* **1977**, *67*, 4086.
31. Abramowitz, M.; Stegun, I. A.; *Handbook of Mathematical Functions* Dover: New York, 1965.
32. Braga, J. P.; *J. Comp. Chem.* **1989**, *10*, 413.
33. Huang, K.; *Statistical Mechanics*; John Wiley & Sons: New York, 1987.
34. Grisenti, R. E.; Schollkopf, W.; Toennies, J. P.; *Phys. Rev. Lett.* **2000**, *85*, 2284.
35. Braga, J. P.; Murrell, J. N.; *Mol. Phys.* **1984**, *53*, 295.
36. Forsythe, G. E.; Malcolm, M. A.; Moler, C. B.; *Computer Methods for Mathematical Computations*; Prentice-Hall: New York, 1977.
37. McCongille, G. T.; Hurly, J. J.; *Metrologia* **1991**, *28*, 375.
38. Berry, K. H.; *Metrologia* **1979**, *15*, 89.
39. Ho, T.; Rabitz, H.; *J. Chem. Phys.* **1988**, *89*, 5614.

Submitted: August 7, 2012

Published online: February 21, 2013